

Thiết kế anten mảng trạm gốc có độ lợi cao, mức búp sóng bên thấp cho hệ thống thông tin 5G dài tầm dưới 6 GHz

TÓM TẮT

Trong bài báo này, một anten mảng có độ lợi cao, mức búp sóng bên thấp được đề xuất cho ứng dụng trạm gốc 5G dưới 6 GHz hoạt động trong băng tần C. Anten này dựa trên thiết kế lưỡng cực điện từ (ME) đã được điều chỉnh, bao gồm hai tấm kim loại hình tam giác, hai tấm kim loại hình chữ nhật, các cột kim loại nối đất, một đầu dò hình L, mặt phẳng đất và đường tiếp điện vi dài. Phần tử anten đơn, với kích thước tổng thể $96 \text{ mm} \times 96 \text{ mm} \times 2.4 \text{ mm}$ (xấp xỉ $1.55\lambda_0 \times 1.55\lambda_0 \times 0.04\lambda_0$ tại 4.9 GHz), đạt băng thông trễ kháng rộng từ 4.50 GHz đến 5.06 GHz với hệ số phản xạ ($|S_{11}|$) dưới -10 dB , và độ lợi cực đại 3.1 dBi . Một mảng tuyển tính 1×8 phần tử lưỡng cực ME được phát triển sử dụng kích thích đồng pha và đồng biên. Cấu hình này mang lại độ lợi cực cao là 13.8 dBi ; tuy nhiên, cũng dẫn đến mức búp sóng bên khá cao là -12.9 dB . Để giải quyết hạn chế này, kỹ thuật giảm biên độ hình thang được áp dụng cho tiếp điện mảng. Các kết quả mô phỏng cho thấy anten mảng cải thiện đáng kể mức búp sóng phụ, đạt dưới -28 dB trong khi vẫn duy trì độ lợi cao 13.6 dBi .

Design of High Gain, Low Side-lobe Level Base Station Array Antenna for 5G-sub 6 GHz communication system

ABSTRACT

In this paper, a high-gain and low side-lobe level array antenna is proposed for 5G sub-6 GHz base station applications operating in the C-band. The antenna is based on a modified magneto-electric (ME) dipole design, comprising two triangular metallic plates, two rectangular metallic plates, grounded vias, an L-shaped probe, a ground plane, and a microstrip feed line. A single antenna element, with overall dimensions of $96 \text{ mm} \times 96 \text{ mm} \times 2.4 \text{ mm}$ (approximately $1.55\lambda_0 \times 1.55\lambda_0 \times 0.04\lambda_0$ at 4.9 GHz), demonstrates a wide impedance bandwidth ranging from 4.50 GHz to 5.06 GHz with a reflection coefficient ($|S_{11}|$) below -10 dB , and achieves a peak gain of 3.1 dBi. A 1×8 linear array of ME dipole elements is developed using uniform in-phase and equal-amplitude excitation. This configuration yields a high peak gain of 13.8 dBi; however, it also results in relatively high side-lobe levels, reaching -12.9 dB . To address this limitation, a trapezoidal amplitude tapering technique is applied to the excitation of the array. The simulated results indicate a significant improvement, achieving a side-lobe level below -28 dB while maintaining a high gain of 13.6 dBi.

Keywords: High gain, side-lobe level, array antenna, 5G-sub 6 communications

1. INTRODUCTION

With the exponential growth of mobile data traffic and the proliferation of smart devices, the evolution of cellular communication technologies toward the fifth generation (5G) has become indispensable. While millimeter-wave (mmWave) technologies have garnered attention due to their large bandwidths, the sub-6 GHz frequency range remains crucial for wide-area coverage, better penetration, and reliable connectivity, especially for 5G macro base station deployments¹⁻³. Consequently, the design of high-performance antenna arrays suitable for 5G-sub 6 GHz applications has emerged as a vital research focus.

Among various antenna technologies, magneto-electric (ME) dipole antennas have demonstrated significant advantages for base station applications. Formed by combining electric and magnetic dipole components, these antennas offer wide bandwidth, stable gain, and low cross-polarization levels. Their inherently symmetrical structure and differential feeding make them well-suited for dual-polarized arrays, which are essential in modern MIMO systems.⁴⁻⁶

Recent works have extended ME dipole designs into planar and low-profile configurations by leveraging printed circuit

board (PCB) technology to enable mass production and ease of integration. Arrays composed of ME dipoles have demonstrated the ability to maintain stable radiation patterns, support beamforming, and achieve wide-angle scanning—capabilities that are essential for dynamic 5G environments. However, most studies have predominantly focused on the mmWave bands, whereas optimized designs for the sub-6 GHz spectrum remain relatively underexplored.

In addition to impedance bandwidth and polarization diversity, two essential performance indicators for 5G base station antenna arrays in the sub-6 GHz band are realized gain and side-lobe level (SLL). High gain ensures that the antenna can support long-distance communication and high data throughput, which are crucial for macrocell coverage and enhanced user experiences in dense urban and rural environments. Meanwhile, low SLL is vital to minimize interference, improve beamforming precision, and enhance signal-to-noise ratio in multi-user MIMO systems.

Recent studies have demonstrated significant improvements in gain performance of ME dipole arrays designed for sub-6 GHz. For example, the dual-polarized array achieved a peak gain of 9.2 dBi across a wide operating band from 3.3 GHz

to 4.2 GHz, while maintaining a compact form factor suitable for 5G base stations¹⁰. Another study introduced a filtering ME dipole antenna with enhanced radiation performance, demonstrating a peak gain of 10.4 dBi and a front-to-back ratio exceeding 20 dB¹¹. These characteristics make such designs favorable for sectorized base station deployment.

Furthermore, the control of side-lobe levels has been a focus in optimizing array radiation patterns. A 4×4 dual-polarized ME dipole array was proposed with a side-lobe suppression of better than -13 dB across the E-plane and H-plane, ensuring minimal leakage of radiated power into undesired directions¹². The incorporation of parasitic elements and advanced feed networks has also contributed to consistent low SLLs while retaining high efficiency¹³.

Maintaining an optimal balance among gain, SLL, and structural simplicity continues to present a fundamental trade-off. Consequently, ongoing research focuses on techniques such as amplitude tapering, optimization of element spacing, and ground plane shaping to further enhance the radiation characteristics of ME dipole arrays operating in the sub-6 GHz band^{14,15}. These innovations are driven by the need to address practical deployment challenges, including wind resistance, manufacturing cost-efficiency, and seamless integration of the array into compact radome structures. Overall, the continuous evolution in ME dipole array design demonstrates promising potential to deliver the desired electrical and mechanical performance needed for next-generation 5G sub-6 GHz base station antennas.

This study presents a high-gain, high-side-lobe suppression magneto-electric (ME) dipole antenna designed for 5G-sub 6 GHz applications, specifically operating at 4.9 GHz within the C-band spectrum. The antenna is excited using an L-shaped probe, which effectively stimulates the ME dipole mode while preserving a low-profile structure suitable for compact deployments. To evaluate its performance in practical scenarios, a 1×8 linear antenna array configuration was implemented and optimized for base station use. Furthermore, by employing trapezoidal excitation techniques, the array achieved a peak gain of 13.6 dBi and exhibited side-lobe levels below -28 dB, indicating excellent radiation pattern control and suitability for high-performance wireless communication systems.

The remainder of the paper is organized as follows. Section 2 provides detailed designs and performance simulations for the single ME dipole antenna. A 1×8 elements linear array design with in phase equal-magnitude and in phase tapering-magnitude feeding are given in Section 3, while some conclusions and future development of are contained in Section 4.

2. SINGLE ANTENNA DESIGN

2.1. Antenna geometry

The antenna's geometry is depicted in Fig. 1. The proposed antenna made up by two dielectric layers which are FR4_epoxy sheet with a relative permittivity of 4.4. The ME dipole is printed on the substrate #1 with a thickness of 1.6 mm and a dimension of $W_{GND} \times W_{GND}$. The antenna consists of four metallic plates, six metallic posts, an L-shaped probe, and a ground plane. Plated through-hole technology was used to create the metallic posts with a diameter of 1.0 mm. A 50 Ohm microstrip line was connected to the vertical portion of the 1.0 mm diameter L-shaped probe. The feeding line was printed on the substrate #2, which has a 0.8 mm thickness.

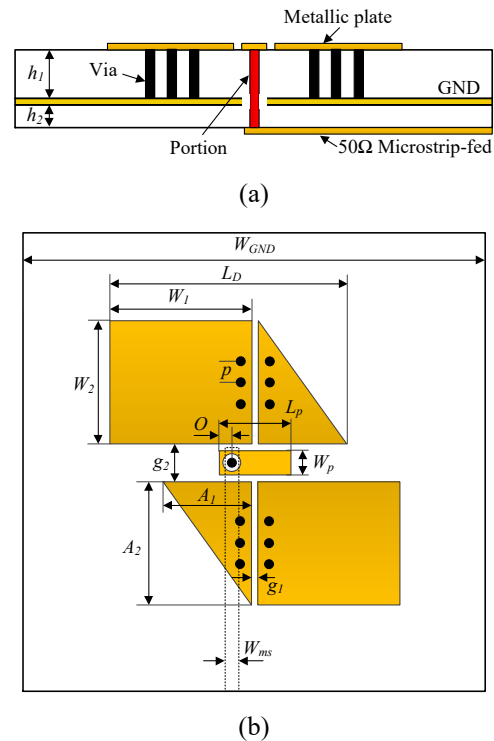


Figure 1. Geometry of the proposed antenna: (a) side view, (b) top view.

2.2. Parameter study

To identify the optimal dimensional parameters of the proposed antenna, it is

essential to initially approximate initial values, including the ME dipole length and the width W_{ms} of the 50-ohm feed line. Subsequently, the resonance frequency is examined based on these initial values and then compared to the intended design frequency. The optimization process is then carried out by analyzing the dimensional parameters of the single element antenna. Specifically, each parameter is varied individually to observe its effect on the resonant frequency, while keeping the remaining parameters constant.

Given a specified center resonance frequency, the length L_d of the ME antenna can be estimated. In practice, the ME antenna's length L_d is initially approximated as half of the free-space wavelength at the center design frequency. Hence, the initial estimate of L_d can be readily computed, yielding a value of approximately 30.6 mm (which corresponds to $\sim 0.5\lambda_0$ at 4.9 GHz). The characteristic impedance Z_0 can be calculated with given the dimensions of the microstrip line as¹⁶.

$$Z_0 = \begin{cases} \frac{60}{\sqrt{\epsilon_{\text{eff}}}} \ln \left[\frac{8h}{w_0} + \frac{w_0}{4h} \right], & \frac{w_0}{h} \leq 1 \\ \frac{120\pi}{\sqrt{\epsilon_{\text{eff}}} \left[\frac{w_0}{4h} + 1.393 + 0.667 \ln \left(\frac{w_0}{4h} + 1.444 \right) \right]}, & \frac{w_0}{h} > 1 \end{cases} \quad (1)$$

where ϵ_{eff} is the relative effective dielectric, w_0 is the microstrip line width, and h is the substrate thickness.

With the characteristic impedance $Z_0 = 50 \Omega$, the feeding line width is calculated as $W_{ms} = 1.49$ mm.

Figure 2 presents the simulated $|S_{11}|$ of a single antenna with calculated L_d and W_{ms} values. It can be observed that the antenna operates at a frequency of 4.91 GHz. However, the impedance matching is not satisfactory. As can be seen from this figure, the antenna can broaden its impedance bandwidth thanks to an extra resonance. To address this issue, the dipole feeding probe position, which is defined as O , will be investigated to optimize the impedance matching as well as the operating bandwidth of n79 frequency band (C-band).

The simulated results presented in Figure 3 indicated that the deep resonance of the single antenna can also be adjusted by changing the feeding position O . This proves that the impedance matching of the single antenna can

be optimized by changing the feeding position of L-shaped probe feed.

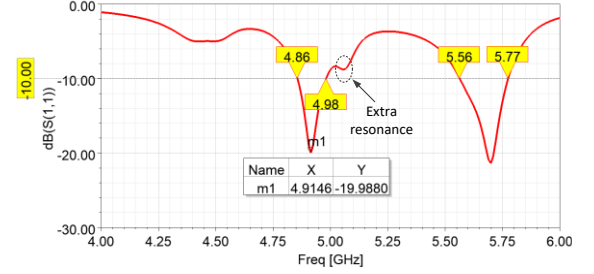


Figure 2. Simulated $|S_{11}|$ of single antenna with initial $L_d = 14.9$ mm.

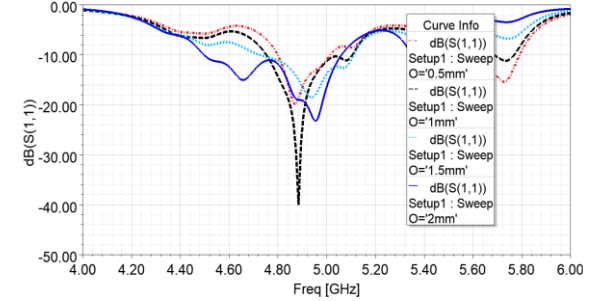
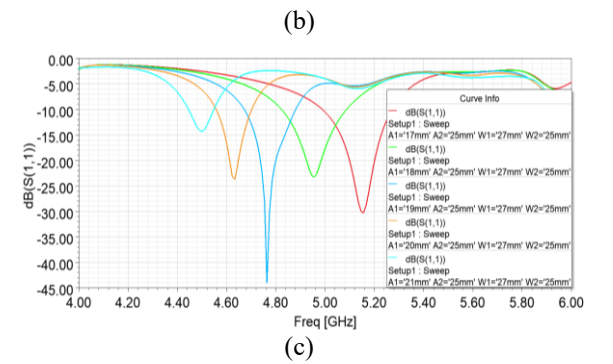
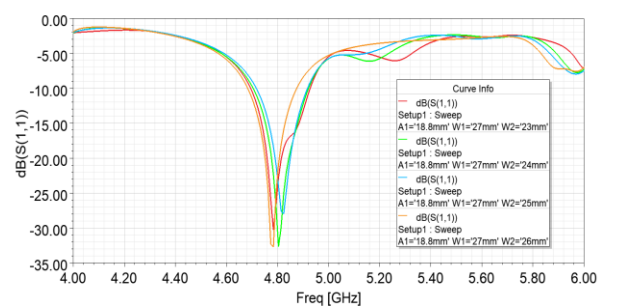
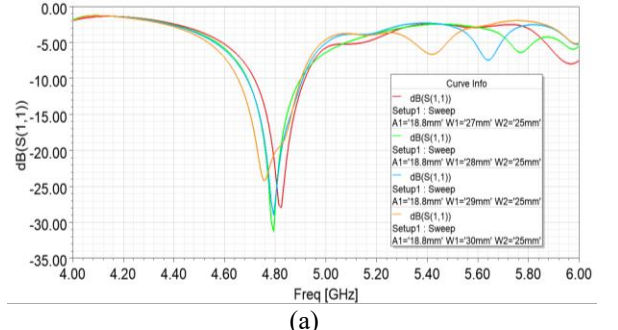


Figure 3. Simulated $|S_{11}|$ of single antenna for different O



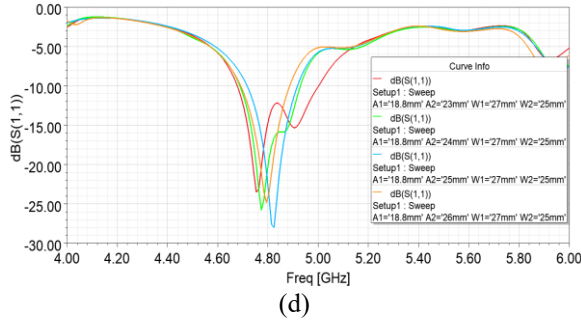


Figure 4. Simulated $|S_{11}|$ of single antenna for different: (a) W_1 , (b) W_2 , (c) A_1 , (d) A_2

Figure 4 presents the $|S_{11}|$ simulated of single ME antenna with different value of W_1 , W_2 , A_1 , and A_2 . As can be observed at Fig. 4(a) and 4(b), the center frequency of single antenna almost did not change when W_1 , W_2 varied. As shown in Fig. 4(c), when A_1 was increased, the center frequency of the single antenna was decreased while this center frequency shifted slightly when A_2 varied as shown in Figure 4(d). This proves that the center frequency of the single antenna can be effectively adjusted by changing the values of A_1 .

The simulated $|S_{11}|$ of final single antenna is shown in Fig. 5. It can be seen that the antenna exhibits a -10 dB impedance bandwidth ranging from 4.50 GHz to 5.06 GHz. Fig. 6 presents the simulated radiation pattern of single antenna in x-z and y-z plane. It is observed that the antenna yielded an omnidirectional in both planes with a peak gain of 3.1 dBi.

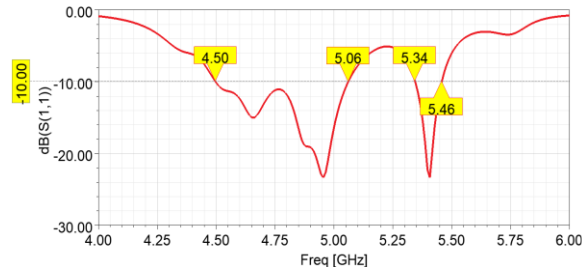


Figure 5. Simulated $|S_{11}|$ of single antenna.

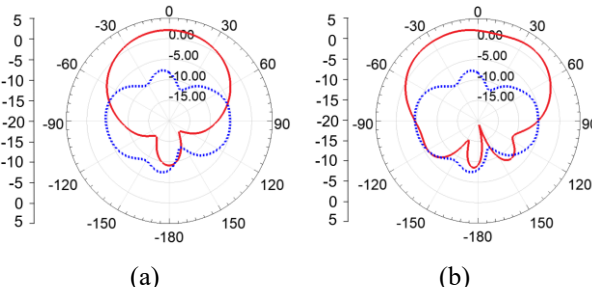


Figure 6. Simulated radiation pattern of the single dipole at 4.9 GHz in (a) x-z plane, (b) y-z plane.

The final design parameters of the single antenna were as follows: $W_{GND} = 96$ mm, $W_1 = 27$ mm, $W_2 = 25$ mm, $A_1 = 18.8$ mm, $A_2 = 23$ mm, $W_{ms} = 1.49$ mm, $L_p = 15$ mm, $W_p = 5$ mm, $g_1 = 1.0$ mm, $g_2 = 7.0$ mm, $O = 2$ mm, and $p = 4.5$ mm.

3. ARRAY ANTENNA DESIGN

In this section, we first analyze the performance of the array by utilizing an in-phase equal-magnitude feeding network. Subsequently, we implement an in-phase tapering-magnitude feeding network to reduce the side-lobe levels of a 1×8 element array antenna. Both feeding networks are designed on FR4 epoxy material with a thickness of 0.8 mm.

3.1. Conventional feeding network

A conventional feeding network consisting of multiple equal T-junction power dividers is employed to achieve in-phase, equal-magnitude excitation for the 1×8 element array antenna. As illustrated in Figure 7, the 1×8 array exhibits a directional radiation pattern in the y-z plane, achieving a peak gain of 13.8 dBi. However, as shown in Figure 8, the array exhibits a relatively high side-lobe level of -12.9 dB.

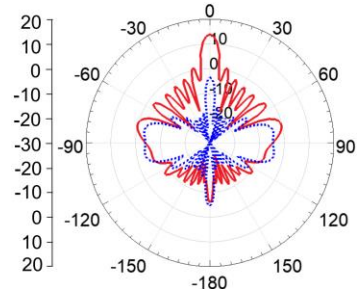


Figure 7. Simulated radiation pattern of 1×8 elements array at 4.9 GHz with an in-phase equal-magnitude feeding (solid line: co-pol, dashed line: cross-pol).

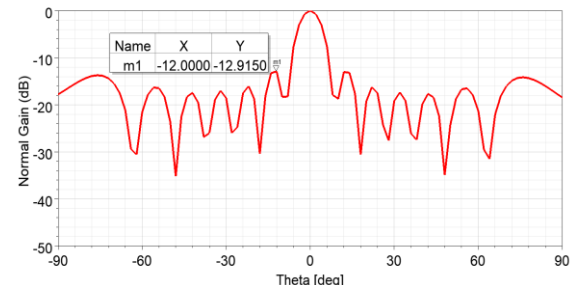


Figure 8. Simulated normal gain of the 1×8 array at 4.9 GHz with an in-phase, equal-magnitude feeding

3.2. Tapering-magnitude feeding network.

In order to reduce the side-lobe, a new magnitude distribution of the excitation, which is type trapezoidal distribution, is designed for the 1×8 elements linear arrays. The feeding network is constructed using a cascade of multiple unequal T-junction power dividers to realize the desired trapezoidal amplitude excitation. The design of the unequal T-junctions is based on impedance transformation principles, in which the characteristic impedances of the microstrip transmission lines are carefully calculated to achieve the desired power division ratios. Quarter-wavelength transmission line transformers are employed for impedance matching between stages. To circumvent fabrication issues associated with extremely narrow microstrip lines-typically required for high impedance values-each power divider incorporates a 50Ω to 25Ω transformation section. Detailed feeding network is illustrated in Figure 9. The magnitude for each element is detailed in Table 1.

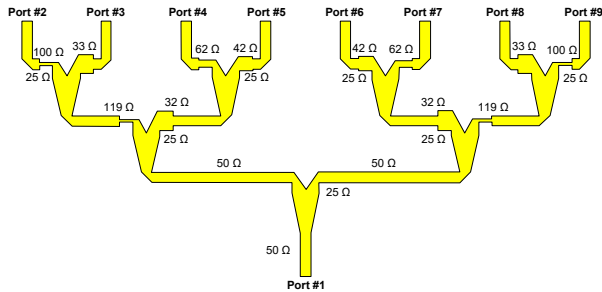


Figure 9. Feeding network of the trapezoidal excitation.

Table 1. Tapering-magnitude excitation for 1×8 ME antenna array.

Element no.	#1	#2	#3	#4	#5	#6	#7	#8
Magnitude	1	3	6	9	9	6	3	1

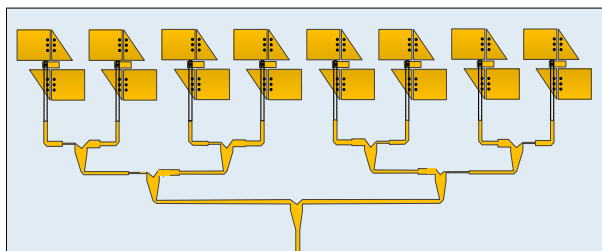


Figure 10. Geometry of 1×8 elements linear array fed by in-phase and tapering-magnitude feeding network.

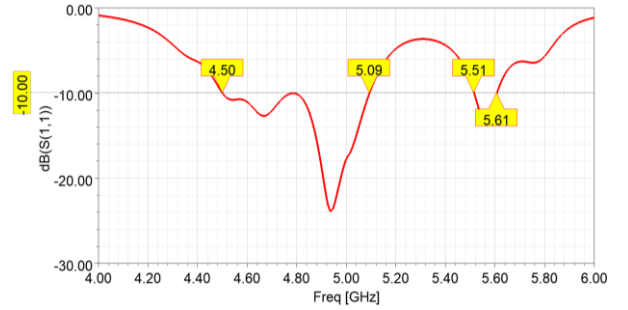


Figure 11. Simulated $|S_{11}|$ of of 1×8 elements array

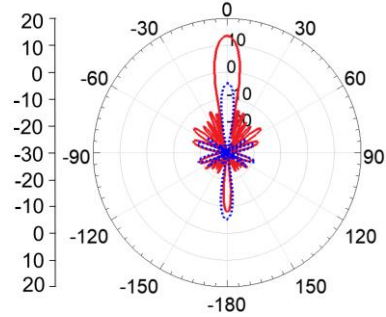


Figure 12. Simulated radiation pattern simulated of 1×8 array at 4.9 GHz (solid line: co-pol, dashed line: cross-pol) with an in-phase trapezoidal feeding

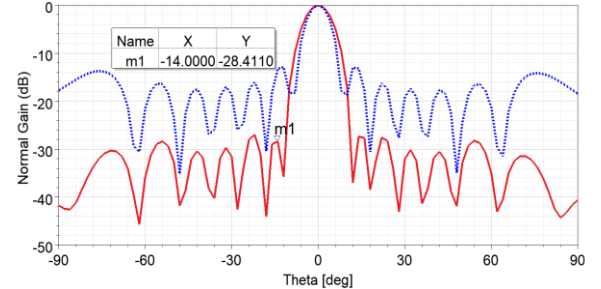


Figure 13. Simulated normal gain of 1×8 elements array at 4.9 GHz with an in-phase trapezoidal feeding

Figure 10 shows the 1×8 elements array incorporated with in-phase and tapering-magnitude feeding network. The array antenna exhibits a -10 dB bandwidth of 509 MHz, ranging from 4.50 GHz to 5.09 GHz, as illustrated in Figure 11. The simulated radiation performance of the array with the trapezoidal excitation is given in Figure 12. As can be observed that the array yielded a gain of 13.6 dBi and a side-lobe of -28.4 dB. These results indicate that the 1×8 elements linear array with the new excitation yields a lightly lower gain, but a significantly lower side-lobe in comparison with the array fed by in-phase equal-magnitude excitation, as depicted in Figure 13.

4. CONCLUSION

A high-gain, low side-lobe level magneto-electric (ME) array antenna has been developed for base station applications operating in the n79 frequency band (C-band) of the 5G sub-6 GHz communication spectrum. The proposed antenna structure **comprises** two rectangular and two triangular metallic radiating elements, six grounded vias, an L-shaped feeding probe, a ground plane, and a microstrip line feed. The single-element antenna **achieves** an impedance bandwidth of 11.4% (ranging from 4.50 GHz to 5.06 GHz) for $|S_{11}| < -10$ dB, along with a peak gain of 3.1 dBi. **Subsequently**, a linear array consisting of 1×8 elements was designed using a conventional feeding network based on multiple equally split T-junctions. This array configuration achieved a high peak gain of 13.8 dBi but suffered from a relatively high side-lobe level (SLL) of -12.9 dB. To mitigate this issue, a modified excitation scheme employing a trapezoidal amplitude distribution was implemented for the linear ME dipole array. Simulation results indicate that the revised configuration achieves a peak gain of 13 dBi and a significantly reduced side-lobe level, which is **below** -28 dB.

Acknowledgments

REFERENCES

1. T. Liu et al., Dual-Wideband Dual-Polarized Magnetoelectric Dipole Antenna for Sub-6 GHz Applications. *IEEE Antennas Wirel. Propag. Lett.*, **2023**, 22(6), 1396-1400.
2. Z. Song and J. Qi. A Novel Dual-Polarized Magnetoelectric Dipole Antenna and Its Array for LTE and 5G Sub-6 GHz Base Station Applications. *Entropy*, **2023**, 25(2), p. 274
3. D. Yang et al. A Novel Differentially Fed Dual-Polarized Filtering Magneto-Electric Dipole Antenna for 5G Base Station Applications. *IEEE Trans. Antennas Propag.*, **2022**, 70(7), 5373-5382.
4. L. Zhao et al. Design of Wideband Dual-Polarized ME Dipole Antenna with Parasitic Elements and Improved Feed Structure, *IEEE Antennas Wirel. Propag. Lett.*, **2023**, 22(1), 174-178.
5. G. Scalise et al. Dual-Polarized Magneto-Electric Dipole for 5G 28 GHz Phased Array Applications, *IEEE Open J. Antennas Propag.*, **2023**.
6. M. Li and K. Luk. Wideband Magneto-Electric Dipole Antenna for 60-GHz Millimeter-Wave Communications, *IEEE Trans. Antennas Propag.*, **2015**, 63(7), 3276-3279.
7. Y. Li and K. M. Luk. A 60-GHz Wideband Circularly Polarized Aperture-Coupled Magneto-Electric Dipole Antenna Array, *IEEE Trans. Antennas Propag.*, **2016**, 64(4), 1325-1333.
8. L. Zhao et al. A Study on Millimeter-Wave Magneto-Electric Dipole Phased Arrays for 5G Dual-Band Applications, *IEEE Trans. Antennas Propag.*, **2022**, 71(3), 2375-2384.
9. D. A. Sehrai et al., Design of High Gain Base Station Antenna Array for mm-Wave Cellular Communication Systems, *Scientific Reports*, **2023**, 13(1), p. 4907.
10. L. Zhao et al. Design of Wideband Dual-Polarized ME Dipole Antenna with Parasitic Elements and Improved Feed Structure, *IEEE Antennas Wirel. Propag. Lett.*, **2023**, 22(1), 174-178.
11. D. Yang et al. A Novel Differentially Fed Dual-Polarized Filtering Magneto-Electric Dipole Antenna for 5G Base Station Applications, *IEEE Trans. Antennas Propag.*, **2022**, 70(7), 5373-5382.
12. Z. Song and J. Qi. A Novel Dual-Polarized Magnetoelectric Dipole Antenna and Its Array for LTE and 5G Sub-6 GHz Base Station Applications, *Entropy*, **2023**, 25(2), p. 274.
13. T. Liu et al. Dual-Wideband Dual-Polarized Magnetoelectric Dipole Antenna for Sub-6 GHz Applications, *IEEE Antennas Wirel. Propag. Lett.*, **2023**, 22(6), 1396-1400.
14. Y. Li et al. Low Sidelobe and High Gain Dual-Polarized Antenna Array for Sub-6 GHz 5G Base Stations, *IEEE Access*, **2021**, 9, 108776-108784.
15. M. Li and K. M. Luk, Analysis of a Wideband Magneto-Electric Dipole Antenna with Low Cross Polarization and High Gain for Base Station Applications, *IEEE Trans. Antennas Propag.*, **2018**, 66(1), 67-76.
16. D. M. Pozar, *Microwave engineering: theory and techniques*, John Wiley & sons, **2021**.